J Mol Model (2008) 14:777–788
DOI 10.1007/s00894-008-0317-9

ORIGINAL PAPER

Structural evidence for lack of inhibition of fish goose-type lysozymes by a bacterial inhibitor of lysozyme

Peter Kyomuhendo · Inge W. Nilsen · Bjørn Olav Brandsdal · Arne O. Smalås

Received: 30 November 2007 / Accepted: 14 April 2008 / Published online: 20 May 2008

Abstract It is known that bacteria contain inhibitors of lysozyme activity. The recently discovered *Escherichia coli* inhibitor of vertebrate lysozyme (Ivy) and its potential interactions with several goose-type (g-type) lysozymes from fish were studied using functional enzyme assays, comparative homology modelling, protein–protein docking, and molecular dynamics simulations. Enzyme assays carried out on salmon *g*-type lysozyme revealed a lack of inhibition by Ivy. Detailed analysis of the complexes formed between Ivy and both hen egg white lysozyme (HEWL) and goose egg white lysozyme (GEWL) suggests that electrostatic interactions make a dominant contribution to inhibition. Comparison of three dimensional models of aquatic *g*-type lysozymes revealed important insertions in the β domain, and specific sequence substitutions yielding altered electrostatic surface properties and surface curvature at the protein–protein interface. Thus, based on structural homology models, we propose that Ivy is not effective against any of the known fish g-type lysozymes. Docking studies suggest a weaker binding mode between Ivy and GEWL compared to that with HEWL, and our models explain the mechanistic necessity for conservation of a set of residues in *g*-type lysozymes as a prerequisite for inhibition by Ivy.

P. Kyomuhendo · I. W. Nilsen
Marine Biotechnology and Fish Health,
Norwegian Institute of Fisheries and Aquaculture,
P.O. Box 6122, 9291 Tromsø, Norway

P. Kyomuhendo · B. O. Brandsdal · A. O. Smalås (✉)
The Norwegian Structural Biology Centre,
Department of Chemistry, University of Tromsø,
9037 Tromsø, Norway
e-mail: Arne.Smalas@chem.uit.no

Keywords Lysozyme · Goose-type · Inhibitor · Vertebrate · Homology modelling · Protein docking

Introduction

The bacterial plasma membrane is surrounded by a peptidoglycan layer, a high molecular weight insoluble polymer of sugars and amino acids forming the rigid layer of the bacterial cell wall. Lysozymes (EC 3.2.1.17) catalyse hydrolysis of the β-glycosidic bond between the C1 of N-acetylmuramic acid (NAM) and the C4 of N-acetyl-D-glucosamine (NAG) in the peptidoglycan, hence their antibacterial activity [1–3]. Gram negative bacteria are considered to be insensitive to lysozyme due to the presence of an outer membrane surrounding the peptidoglycan, which may function as a physical barrier preventing lysozyme from reaching the peptidoglycan. This view has however been challenged through ultrastructural studies on the effect of lysozyme on *Escherichia coli* [4]. Three families of lysozymes have been identified in animals: types *c* (chicken), *g* (goose) and *i* (invertebrate) [1–3, 5–10]. *c*-Type lysozyme proteins and gene organisations are highly conserved in vertebrates as well as in arthropods [3], while *i*-type lysozymes are similarly conserved in invertebrates [11, 12]. In contrast, the *g*-types found in terrestrial and aquatic vertebrates, and in marine invertebrates, are much more divergent [7, 8]. Typical *g*-type lysozymes (~20–22 kDa) are significantly larger than *c*- and *i*-type lysozymes (11–15 kDa) and there are no extensive sequence homologies between the three types. Nevertheless, the three dimensional (3D) structures of *c*-, *g*- and even phage-type lysozymes are quite similar to each other [13]. The *i*-type lysozymes in particular, but also a *c*-type lysozyme variant in Rainbow trout, differ from other animal

lysozymes by having significant antibacterial activity against Gram negative bacteria [10, 14].

It was discovered that bacteria produce proteins with strong inhibitory effects on lysozymes, i.e. the periplasmic inhibitor of vertebrate lysozyme (Ivy) from the Gram negative *E. coli* [15], and the extracellular streptococcal inhibitor of complement (SIC) from the Gram positive *Streptococcus pyrogenes* [16]. Several Ivy homologues have since been identified and studied [17, 18]. Both inhibitors are strategically positioned to protect their respective vital peptidoglycans from lysis by lysozyme. Although knock-outs or deletion mutants have demonstrated that these inhibitors have no essential function per se, both inhibitors were shown to be important for survival when exposed to lysozymes alone or to lysozyme-containing environments [19, 20]. SIC displays a surprisingly broad range of inhibiting activities besides lysozyme inhibition [16, 21]. In contrast, Ivy has so far been reported to inhibit only lysozymes, i.e. vertebrate *c*-type lysozymes (with varying efficiency) as well as phage lysozyme and goose *g*-type lysozyme [15, 22], but not *i*-type or *g*-type lysozyme from two marine invertebrates [8]. Periplasmic inhibitors of hen egg white lysozyme (HEWL) have recently been isolated from *Salmonella enteritidis*, *Klebsiella pneumoniae* and *Shigella flexneri* [17, 23]. The 3D structures of *E. coli* Ivy alone or in complex with HEWL, and that of an Ivy homologue in *Pseudomonas aeruginosa* also in complex with HEWL, were recently published [18]. This latter work by Abergel and co-workers also confirmed the presence of a protein family containing a conserved loop motif. The crystal structure of the Ivy-HEWL complex shows that Ivy effectively blocks the active site by inserting a loop into the D–E substrate binding sites. The loop comprises the CKPHDC motif common to all Ivy homologues, with the H60 at its centre making hydrogen bonds with the two main catalytic residues E35 and D52 in HEWL. Ivy is active as a dimer in *E. coli* but acts as a monomer in *P. aeruginosa* [15, 18].

The availability of the crystal structure of the Ivy-HEWL complex motivated us to investigate the potential for employing structural models to predict binding of Ivy to various lysozymes, particularly the divergent *g*-type lysozymes. The reason for this is that Ivy clearly inhibits the vertebrate goose lysozyme but fails to inhibit the corresponding *g*-type lysozyme in a marine invertebrate [8, 22]. A number of fish *g*-type enzymes have been discovered and analysed since 2001 but their possible interaction with Ivy or their 3D structures have so far not been addressed.

Lysozymes play a significant role in the first line of defence against bacterial infections, and we propose that bacterial inhibitors of this host defence mechanism may be targets for future anti-infective compounds. Thus, elucidation of the molecular interactions between lysozymes and Ivy (or other inhibitors) are of importance.

Here, we report structural models as evidence of binding of Ivy to goose *g* lysozyme, although more weakly than to hen *c* lysozyme. Furthermore, a proposed required conservation of a set of residues, which is not present in fish *g* lysozymes, for binding to Ivy, and the consequent predicted lack of inhibition by Ivy was verified by enzyme assays.

Materials and methods

Lysozyme assay

Lysozyme activity of 0.5 μg HEWL (Sigma, St. Louis, MO) and recombinant salmon *g*-type lysozyme [24] was measured as previously described [10] using lyophilised *Micrococcus lysodeikticus* (Sigma) cells resuspended at 0.2 mg/ml in sodium acetate buffer (pH 5.2) by monitoring the continuous change in absorbance at 450 nm in a reaction carried out at room temperature. The assay was repeated in the presence of 1 or 2.5 μg Ivy [22] with similar absorbance readings.

Multiple sequence alignment and phylogenetic analysis

G-type lysozyme sequences were retrieved from protein sequence databases such as UniProt [25] and aligned using the Tcoffee multiple sequence alignment program [26] with default settings. The sequences included Goose (*Anser anser*) P00718, Common carp (*Cyprinus carpio*) Q8JFR1, Zebra fish (*Danio rerio*) Q6DH80, Chinese perch (*Siniperca chuatsi*) Q5XU03, Japanese flounder (*Paralichthys olivaceus*) Q90VZ3, Atlantic cod (*Gadus mohua*) Q1M163, Orange-spotted grouper (*Epinephelus coioides*) Q90X99 and Fugu (*Takifugu rubripes*) P61133. The expressed sequence tag (EST) DW555874 for Atlantic salmon (*Salmo salar*) was retrieved from the EST data bank (dbEST) [27]. A sequence identity matrix was then computed with BioEdit [28] (see Table 1). Tcoffee builds a progressive alignment by adding one sequence after another to the alignment and compares segments across the entire sequence set. Based on this alignment, phylogeny was estimated by the neighbor-joining (NJ) method [29] of clustering in the PHYLIP program [30]. Bootstrap analysis [31] was used, with 1,000 replicates to test the relative support for branches produced by the NJ analysis.

Homology model building

Models based on a local alignment between template (PDB [32] entry: 153 L) and target sequence, were built using the ICM [33] program package. The programs PSQS (http://

Table 1 Sequence identity matrix of goose egg white lysozyme (GEWL) and fish *g*-type lysozymes

Sequence	Catfish	Goose	Carp	Zebra fish	Salmon	Rainbow trout	Chinese Perch	Japanese flounder	Cod	Orange spotted grouper	Fugu
Catfish	ID	0.65	0.68	0.72	0.67	0.67	0.55	0.51	0.59	0.52	0.52
Goose	0.65	ID	0.57	0.59	0.56	0.55	0.51	0.48	0.56	0.49	0.51
Common-carp	0.68	0.57	ID	0.71	0.57	0.56	0.52	0.50	0.56	0.51	0.51
Zebra fish	0.72	0.59	0.71	ID	0.69	0.68	0.53	0.50	0.54	0.52	0.51
Salmon	0.67	0.56	0.57	0.69	ID	0.94	0.51	0.50	0.55	0.51	0.49
Rainbow trout	0.67	0.55	0.56	0.68	0.94	ID	0.50	0.50	0.55	0.52	0.48
Chinese-perch	0.55	0.51	0.52	0.53	0.51	0.50	ID	0.74	0.66	0.87	0.60
Japanese-flounder	0.51	0.48	0.50	0.50	0.50	0.50	0.74	ID	0.59	0.72	0.59
Cod	0.59	0.56	0.56	0.54	0.55	0.55	0.66	0.59	ID	0.64	0.56
Orange-spotted grouper	0.52	0.49	0.51	0.52	0.51	0.51	0.87	0.72	0.64	ID	0.59
Fugu	0.52	0.51	0.51	0.51	0.49	0.48	0.60	0.59	0.56	0.59	ID

www1.jcsg.org/psqs/), VERIFY_3D, ERRAT and ProCheck (http://nihserver.mbi.ucla.edu/SAVS/) were applied to evaluate the quality of the modelled structures [34–38] (Table 2). The verification methods fall into two major classes: one focusing mainly on local environment (PSQS and VERIFY_3D), and the other on local geometry (ERRAT and PROCHECK). The environment-oriented methods PSQS and VERIFY_3D gave scoring values that were approximately similar to those of the template (Table 2). The scoring values of VERIFY_3D and ERRAT are in percentages, and should in general be as high as possible. For the geometry-oriented methods, the scoring differences between the models and the template were more varied in ERRAT than in PROCHECK (Table 2). The Ramachandran plots for the models (not shown) showed that the main-chain dihedral angles were all within acceptable ranges. The quality tests indicated that we have models of sufficient quality, and that they can be used as tools to analyse the scope of inhibition activity (if any) of Ivy on *g*-type lysozymes, particularly those of fish species.

Docking

The Ivy inhibitor protein (PDB entry: 1XS0) was docked into the active site of GEWL using the PatchDock server (http://bioinfo3d.cs.tau.ac.il/PatchDock/). PatchDock uses a molecular docking algorithm based on shape complementarity principles [39]. All dockings were carried out using the restraints that the catalytic Glu of lysozyme and the His60 of Ivy should interact. The recommended clustering RMSD value of 4.0 Å was used. Based on geometric shape complementarity score, the best complex was chosen from the solutions list returned. Deep view (version 3.7) [40] was used for energy minimisation and to identify interaction types. The best ranked solution was further refined using molecular dynamics (MD) simulations.

Molecular dynamics simulation

After constructing the Ivy–GEWL complex, minimisation and MD simulations were carried out using the AMBER program package [41] with the modified parm99 force field. Water molecules were added to the complex with a 15 Å buffer from the edge of the box and described according to the TIP3P model. Counter-ions were added to obtain a neutral system. Prior to MD simulations, the system was minimised using 2,500 steps of steepest decent and 2,500 steps of conjugate gradients first with a positional restraint of 50 kcal mol^{-1} $Å^{-2}$ on protein heavy atoms. This was repeated with a restraint force of 10 kcal mol^{-1} $Å^{-2}$ and finally removed in the last run. The temperature was slowly

Table 2 Quality scores of fish *g*-type lysozyme models using different quality control programs (http://nihserver.mbi.ucla.edu/SAVS/) and (http://www1.jcsg.org/psqs/)

Structure	VERIFY_3D[a]	ERRAT[b]	ProCheck[c]	PSQS[d]
153L (template)	100	97.7	94.9	−0.2309
Q8JFR1	93.6	84.8	84.5	−0.1312
Q1M163	99.5	87.7	87.7	−0.2875
Q90VZ3	98.5	83.9	83.5	−0.2924
P61133	100	90.3	87	−0.3021
Q90X99	100	85.4	83.2	−0.2868
Q5XU03	100	94.4	84.1	−0.3074
DW555874	100	91.2	85.7	−0.2148
Q6DH80	93.33	88.9	87.3	−0.2313

[a] Percentage of residues with average 3D-1D score > 0.2
[b] Percentage of the protein for which the calculated error value falls below the 95% rejection limit
[c] Percentage of residues with Φ and Ψ conformational angles in the 'most favoured regions' of the Ramachandran plot
[d] The average value for the PSQS scores of a representative set of PDB structures is −0.27 and most structures have a PSQS less than −0.1

raised to the target temperature (300 K) followed by a 500 ps equilibration period. The equilibrated complex was then simulated for 1.5 ns in the isothermal-isobaric ensemble (300 K and 1 atm). Temperature and pressure were maintained using the Berendsen coupling algorithm [42]. A non-bonded cutoff of 8 Å was used and the Particle-Mesh-Ewald method [43] was used to handle long-range electrostatics. SHAKE [44] was used to constrain bonds involving hydrogens, allowing a time step of 2 fs.

Results and discussion

Lysozyme inhibition assay

The previously reported apparently contradictory effects of Ivy on *g*-type lysozymes from goose (inhibition) and from the marine invertebrate *Oikopleura dioica* (no inhibition) [8, 22], has been interpreted to reflect some extent of structural variation within this class of lysozymes. It was thus of interest to investigate the effect of Ivy on aquatic vertebrate *g* lysozymes from fish representing a third "subclass" of these enzymes. We have very recently produced and studied a recombinant *g*-type lysozyme from Atlantic salmon that shows low-temperature activity and high heat tolerance [24]. Here, the enzyme was further tested for its bacterial cell wall hydrolysis in the presence of Ivy. Previous studies have shown that Ivy gave complete inhibition of HEWL enzyme activity when equimolar concentrations were used [15]. The results in Fig. 1 show that, while HEWL is inhibited by a two-fold higher concentration of Ivy, no such inhibitory effect is observed for the salmon *g*-type lysozyme. Increasing the Ivy concentration by a further 2.5 fold did not change the result. In the following, we attempt to rationalise the observed lack of inhibition on a structural level, and to investigate whether this should be expected to be a general trend for fish *g*-type lysozymes.

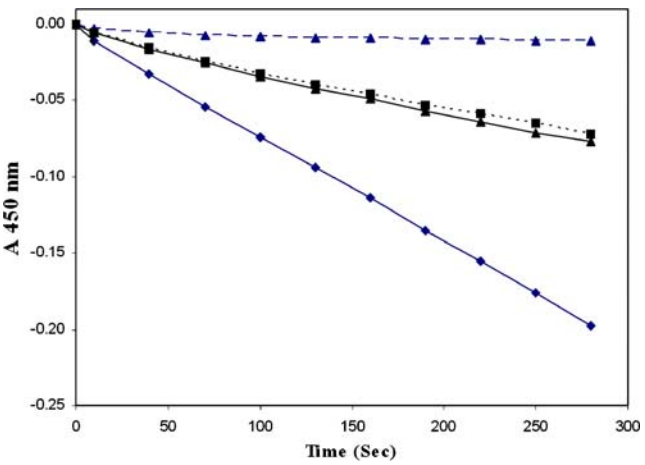

Fig. 1 Lysis of *Micrococcus lysodeikticus* cell suspension by hen egg white lysozyme (HEWL; *diamonds*) and recombinant salmon g-type lysozyme (*triangles*) in the absence (*filled symbols*) or presence (*open symbols*) of the bacterial inhibitor of vertebrate lysozyme (Ivy)

Sequence relationships between g-type lysozymes

Previous studies have shown sequence relationships between *g*-type lysozymes from invertebrates to mammals [7, 8]. Sequence identities between known *g*-type lysozymes range from 21.1% (*Oikopleura*-1 and Human-1) to 96% (GEWL and Black-swan). A phylogenetic tree showing molecular evolutionary relationships between 22 *g*-type lysozymes (Fig. 2) demonstrates that there are two main clades: an invertebrate and a vertebrate clade. The major vertebrate clade is further divided into four subclades (two terrestrial and two aquatic); a mammalian and an avian subclade, and two fish subclades. In the two latter subclades, one consists of freshwater species or species spawning in freshwater, while the second subclade represents a mix of marine, marine-spawning and freshwater species. Eight of the fish *g*-type lysozymes were selected for further analysis in an effort to investigate possible interactions with Ivy.

Structural comparison of *g*-type lysozymes

The structure-based sequence alignment comparing fish *g*-type lysozymes with GEWL shows a high degree of conservation in the overall structure (Fig. 3). The primary structure of the selected aquatic lysozymes apparently resembles the well characterised GEWL α+β fold [13, 45, 46]. The best conserved parts are found in regions that constitute the core of the enzymes and make up the extended groove involved in substrate binding, including the 'catalytic' glutamic acid (E73), the triple-stranded β-sheet and the linker helix α6. The loops connecting secondary structure elements in lysozymes from goose and from fish species in the phylogenetic freshwater-subclade are identical in lengths. The longer loops connecting α5 and β1, β1 and β2 and β3 and α6 seem to be the main difference distinguishing the remaining fish *g*-type lysozymes. Three conserved regions are found in the protein core. These are situated at the end of the 'catalytic' helix, in the first and third β-sheets, in the second hairpin loop of the β-sheet and subsite C (V96, D97, H101, I119 and Y147 in GEWL) with the exception of Fugu lysozyme, which has a substitution V96I. Only cod lysozyme has insertions between the buried 'catalytic' helix α5 and β1. More insertions are observed in the first hairpin loop of the β-sheet and between the β domain and the C-terminal lobe of the α-domain in Orange-spotted grouper, Chinese perch

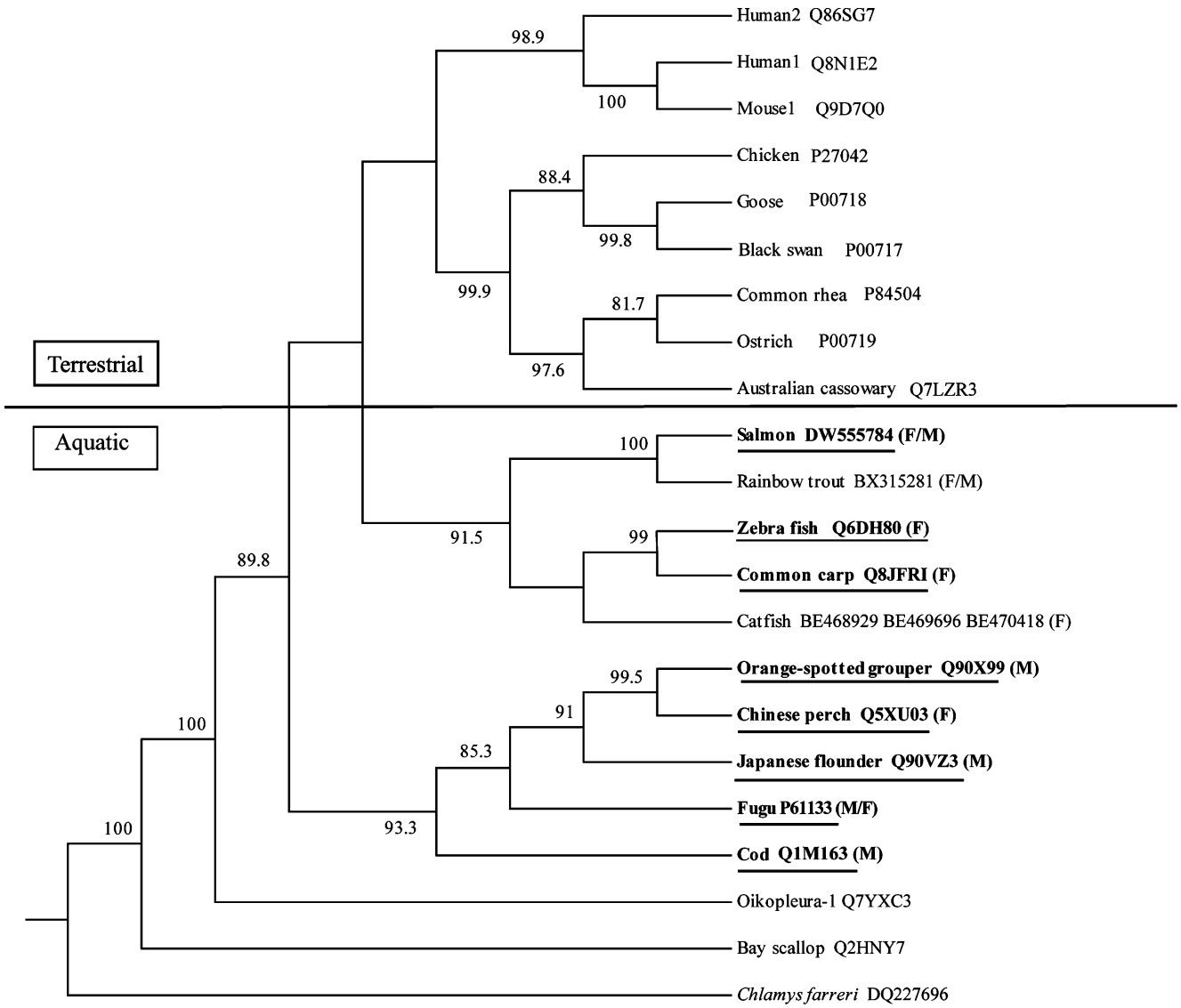

Fig. 2 Phylogenetic tree based on the unambiguously aligned portion of the amino acid sequences of selected *g*-type lysozymes. Sequences used later for modelling are highlighted and underlined. The percent of bootstrap replications (1,000) supporting each branch is shown. Bootstrap values below 60% are not shown. The common name and accession number of the respective fish species and their aquatic environment is indicated (*F* freshwater, *M*: marine); aquatic environment for spawning is indicated first for migrating species

and Japanese flounder *g*-type lysozymes. Fugu lysozyme also has insertions between the β domain and the C-terminal lobe of the α-domain. All but the cod lysozyme have substitutions in the substrate binding site B (N122, F123) when compared to GEWL. A conservative F123Y substitution is observed only for zebrafish, with substitutions at N122 exhibited by all others. Still in comparison to GEWL, other substitutions at active site residues are at D86P in carp lysozyme and at G90A in Orange-spotted grouper and Japanese flounder lysozymes.

The variations in primary structure at the N-terminus have two probable explanations. The first is the species and tissue of origin and the second is the presence of signal peptides in the salmon and zebrafish *g*-type lysozymes [7, 24]. C-terminal variations occur mostly due to insertions, e.g. in Fugu, Orange-spotted grouper, Chinese perch and Japanese flounder *g*-type lysozymes.

Structural models of fish *g*-type lysozymes from Atlantic cod, Common carp, Japanese flounder, Zebrafish, Chinese perch, Orange spotted grouper, Takifugu rubripes and Atlantic salmon were built using the crystal structure of GEWL (PDB entry; 153L) as a template. According to standard evaluation criteria, the quality of the models is generally good. Root-mean-squared deviations (RMSD) for main chain Cα atoms between each of the modelled fish *g*-type lysozymes and GEWL range from 0.49 to 1.5 Å. Areas where large differences are observed between modelled structures are illustrated in Fig. 4. The largest RMSD on aligned Cα atoms was found between GEWL and Chinese perch, due mainly to differences in loop regions.

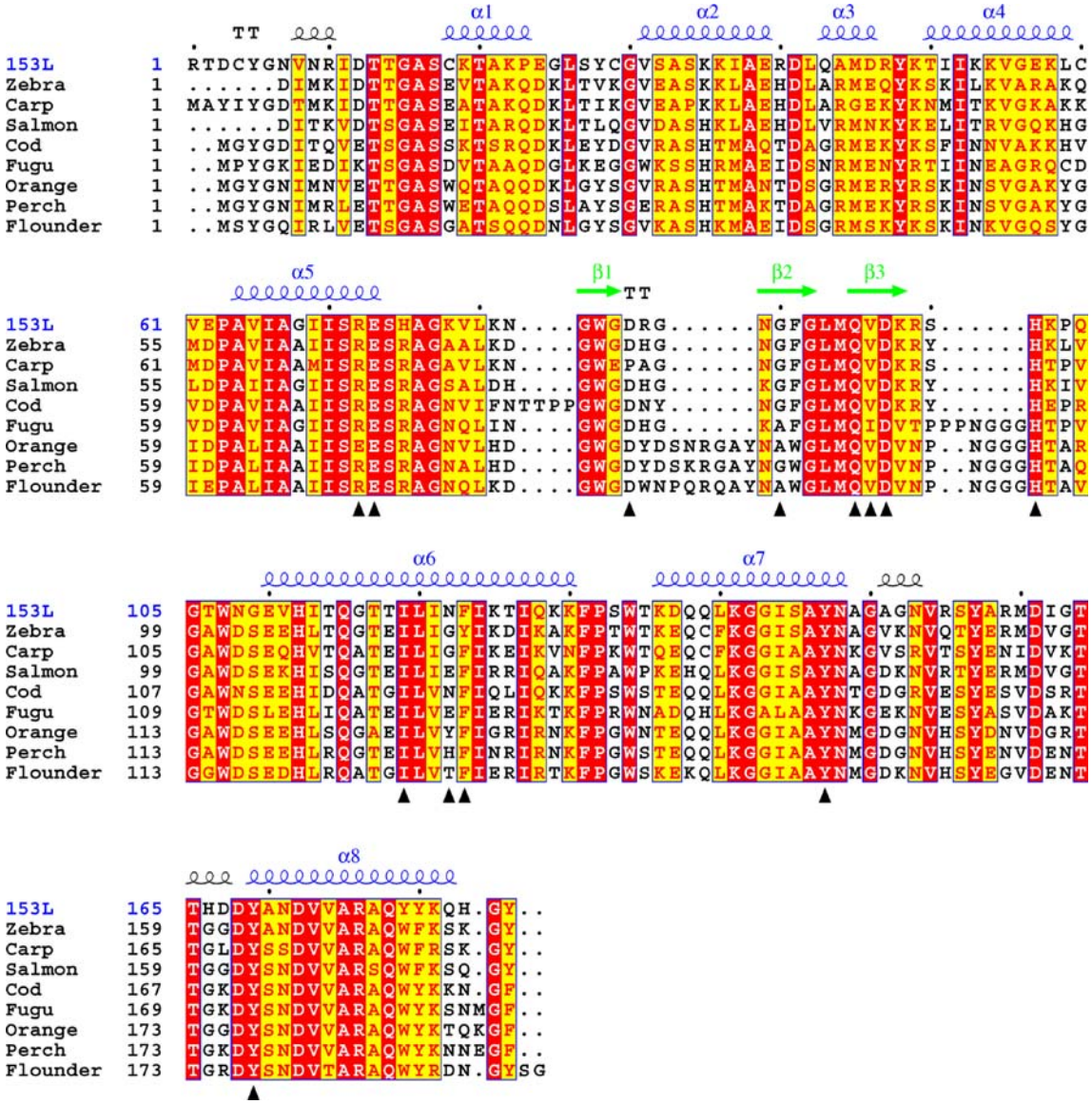

Fig. 3 Sequence comparison of goose egg white lysozyme (GEWL) and some fish *g*-type lysozymes based on overall structural correspondence. Secondary structures for GEWL are shown as *blue spirals* for α-helices and marked α1–α8, while β-sheets are depicted as *green arrows* and marked β1–β3. Predicted signal sequences were removed for Salmon and Zebra fish sequences. *Red* and *yellow* backgrounds indicate identical and similar residues respectively. *Dots* Gaps introduced for optimal alignment, ▲ main active site residues in GEWL

Ivy and its interactions with GEWL

To date, the 3D structure of two complexes where Ivy is bound to lysozyme have been determined, both with HEWL (PDB entries 1GPQ and 1UUZ). Previous inhibition studies have shown that Ivy effectively blocks the activity of GEWL but not of *g*-type lysozyme from the marine invertebrate *O. dioica* [8, 22]. Our finding of no functional inhibition of salmon *g* lysozyme by Ivy is however no evidence for a general lack of inhibiting interaction between fish *g*-type lysozymes and Ivy. Thus, we aimed to define the structural requirements for binding between Ivy and any *g*-type lysozyme, and from this make predictions about interactions with fish *g*-type lysozymes. In order to address these issues, a 3D model structure of Ivy bound to GEWL was constructed using automatic and manual docking procedures. Protein–protein docking can be challenging, particularly when little structural information about the binding sites is available. Several crystal structures of GEWL are available, providing information on the active site and substrate binding sites. Comparison with HEWL shows that the catalytic Asp is lacking in GEWL, while the catalytic Glu is conserved. Furthermore, the crystal structure of Ivy bound to HEWL provides information on which residues promote complex formation on both Ivy and HEWL. Detailed analysis of the Ivy-HEWL

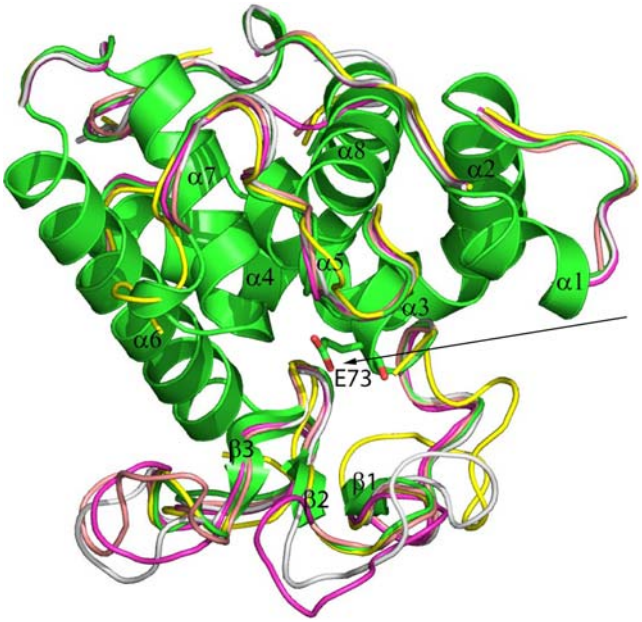

Fig. 4 Cartoon ribbon diagram depicting the superimposed backbone folds of GEWL (*green*), cod (*yellow*), flounder (*magenta*), orange-spotted grouper (*light-grey*) and fugu (*light-brown*) g-type lysozymes. α1–α8 and β1–β3 refer to α- helices and β-sheets, respectively, on GEWL. Highly conserved secondary structure elements are shown for GEWL, and loops only are shown for the models. *Arrow* Active site cleft of GEWL blocked by CKPDHC loop on Ivy. E73 is the main catalytic residue in GEWL

complex reveals that the CKPHDC loop of Ivy blocks the active site of lysozyme. The central His of this loop interacts with the conserved catalytic Glu of lysozyme, and the Ivy–GEWL model was constructed by requiring the presence of this particular interaction. Several docked solutions were retrieved using the PatchDock server and, after visual inspection of the five best solutions, the highest ranked was chosen for further investigation. This complex contained some close contacts, and the model was therefore further relaxed using energy minimisation and MD simulations. The last structure after MD simulations was defined as the final model of the Ivy-GEWL complex, and used for further analysis.

Ivy was also docked to HEWL (using the atomic coordinates from the crystal structure) in order to evaluate the performance of the automatic docking by PatchDock, thus providing validation of the procedure used to build the Ivy–GEWL complex. Several solutions were again obtained with the same docking parameters as for GEWL. However, comparison of the top ranked solutions with the crystal structure showed that only the highest ranked solution had an acceptable agreement with experimental structure. This model has an RMSD of 1.5 Å when compared to the crystal structure (using all heavy atoms), while the second and third ranked solutions have RMSD values of 3.3 and 12.0 Å, respectively. Figure 5 shows the best docked model superimposed onto the crystal structure. It is encouraging that a near-native structure appears as the best solution from the automated docking procedure.

Analysis of the Ivy-GEWL complex reveals that Ivy is bound in a different orientation when compared the experimental structure with HEWL. GEWL has roughly 60 more amino acids, and two regions in particular exclude Ivy from binding in the "HEWL" orientation. These are colored red in Fig. 6, which presents GEWL superimposed with HEWL. Figure 7 shows the model of Ivy–GEWL after MD simulations, and inspection of the protein–protein interface reveals several ionic interactions. Indeed, the crystal structure of Ivy–HEWL already suggests that electrostatic interactions may be important when forming the protein–protein complex. Both sides of the CKPHDC loop of Ivy are anchored to HEWL through favourable ionic interactions. Residues in the CKPHDC loop of Ivy are involved in two ionic networks at the interface in the HEWL complex, whereas only one is observed in the modelled GEWL complex. The central His is placed firmly between the catalytic Glu and Asp in the HEWL complex, but a weaker interaction may be anticipated in GEWL, as this enzyme lacks the Asp. The Ivy–GEWL complex does not have salt bridges on either side of CKPHDC as seen for

Fig. 5 Docking quality assessment by superimposition of the docked Ivy-HEWL complex (*cyan*) onto its corresponding crystal structure (*green*)

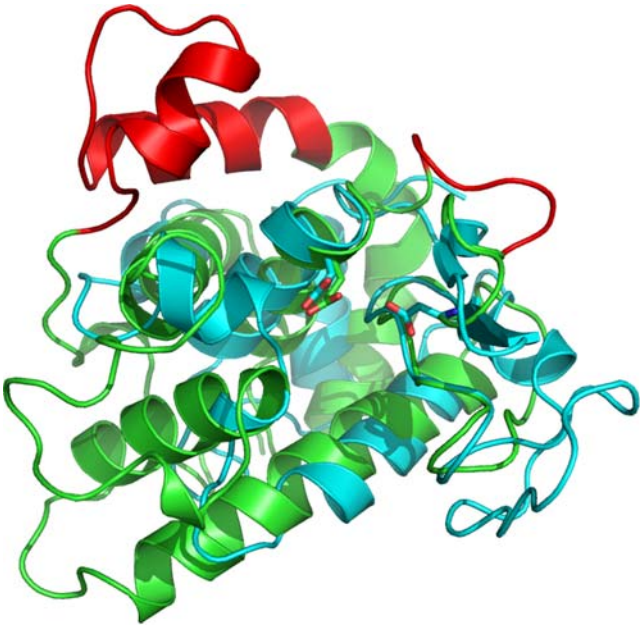

Fig. 6 GEWL (*green*) superimposed onto HEWL (*cyan*). Areas in the GEWL structure with a negative impact on binding to Ivy are presented in *red*. Catalytic residues are shown as *sticks*

HEWL, suggesting that this loop is better anchored in the latter. A consequence of this should be continued inhibition of HEWL rather than of GEWL at lowered concentrations of Ivy, as previously demonstrated by functional testing in enzyme assays [22]. The Lys and Asp residues in the CKPHDC loop also interact with Arg114 in lysozyme, adding further support to the strong binding of Ivy to HEWL. There are, however, residues more distant to the principal interaction site forming well-defined hydrogen bonding and charge–charge interactions in the Ivy–GEWL complex. Hence, the constructed model appears to have optimised electrostatics at and around the protein–protein interface, suggesting a strong inhibition of the goose lysozyme by Ivy. Shape complementarity of the two proteins adds further support to the inhibition potential of Ivy.

Lack of inhibition of fish *g*-type lysozymes by Ivy

GEWL has primary sequence identities ranging from 49 to 58% with selected fish *g*-type lysozymes, and the structural alignment in Fig. 3 revealed a high degree of conservation between the sequences. GEWL is therefore considered as a suitable template for investigating possible Ivy-inhibition of selected lysozymes from fish. Automated docking of Ivy to the target lysozymes was initially tried using the PatchDock server, but no low energy solutions were retrieved. In order to examine possible causes of the failure to obtain docked models, the modelled aquatic lysozymes were superimposed onto the Ivy–GEWL. Protein–protein contacts in a 5 Å radius at the interface of the Ivy–GEWL complex are formed by 18 residues in GEWL, 8 (P23, E24, R40, H75, K78, R87, H166 & D167) of which are exclusively substituted in fish *g*-type lysozymes and occur in conserved regions of the molecule. The three active site residues at the interface, E73, D86 and Q95, are fully conserved in all the fish lysozyme sequences except for D86P in carp lysozyme.

Steric hindrance

Superimposition of the modelled fish lysozymes onto the Ivy–GEWL complex shows severe loop collisions caused by substitutions and insertions of amino acids with different properties. The GEWL-to-fish lysozyme substitutions P23Q, H75R, K78N and R87W are responsible for close contacts with Q65, E87, and C57 or C62 in Ivy, in four of the models (perch and fugu, or cod and flounder, respectively).V79 makes clashes in the cod model and the substitution V79Q is responsible for structural collisions in the model complexes with Ivy for fugu and flounder *g*-type lysozymes. In salmon and zebrafish lysozymes D86 overlaps with Ivy's D61 and C62, whereas only C62 is involved in the fugu and cod counterparts. The D86P and G85E substitutions occurring only in carp *g*-type lysozyme, are responsible for the close contacts with C62 and H60, respectively. The substitution G90A, where it occurs in grouper, fugu and flounder lysozymes, clashes with H60. Q95 on the other hand is invariant across all models and overlaps with H60. In the grouper lysozyme, G88D and K19Q clash with C62 and G63 and A30 in Ivy, respectively, while insertions S87, N88 and R89 collide with K58, P59 and C62, H60 and A56 and C57. Insertions S87 and K88 clash with C62 and K58 and H60, respectively, in the Chinese perch model. The flounder enzyme has the P87 insertion as well as the D167R substitution that clash with T37 and K34, respectively. This account of steric impediments provides further testimony to the fact that Ivy may not inhibit known fish *g*-type lysozymes.

Electrostatic complementarity

The salt bridges formed in the Ivy–HEWL and Ivy–GEWL complexes are shown in Table 3. Out of the five GEWL residues involved in ion-pairs with Ivy, four (E24, H75, K78 and D167) are substituted in fish *g*-type lysozymes. This points to a possible loss of specific interaction between the models and Ivy, and could be yet another reason why Ivy has no inhibitory effect on these fish lysozymes. Electrostatic fields around the surface of proteins play an important role in molecular recognition and binding as verified by a number of studies [47]. Electrostatic surface potentials of Ivy and some fish *g*-type lysozymes were calculated using the Delphi program [48] (Fig. 8). In addition to the specific interactions, negative charges on E35 and D52 in HEWL and E73 in GEWL create a

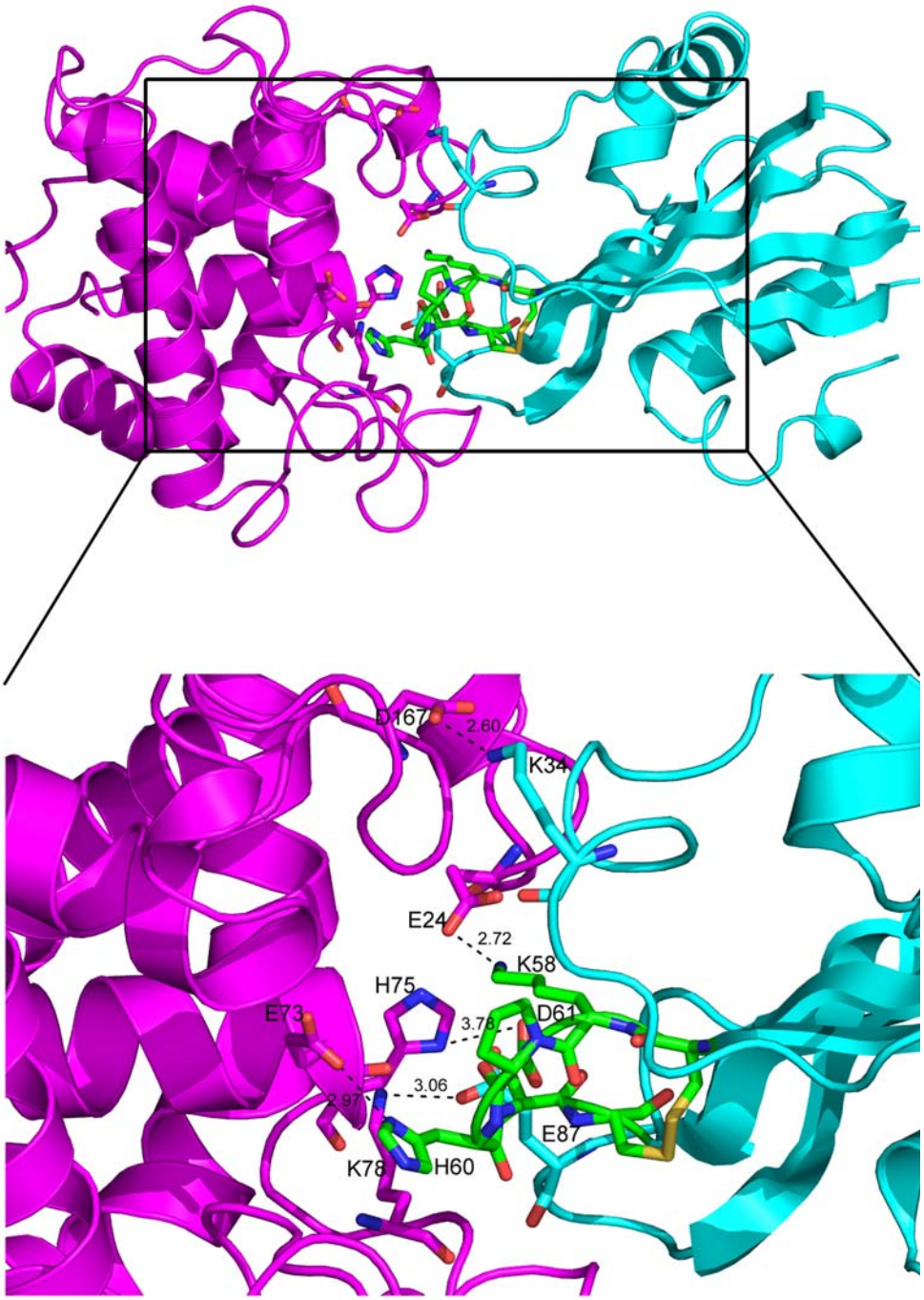

Fig. 7 Ivy (*cyan*) docked in GEWL (*magenta*) and a close-up of the interacting areas showing salt bridges and corresponding distances (Å). The CKPHDC loop on Ivy is represented as *green sticks*. The conserved catalytic glutamate and ion pair forming amino acids in GEWL substituted in fish *g*-type lysozymes are represented as *magenta sticks*

negative electrostatic environment in the entire substrate binding crevice. This negative electric field enhances efficient binding of ligands (substrates) containing a positively charged side chain or group such as H60 on Ivy. Similarly, a surface topography enabling substantial areas of two interacting surfaces to approach each other closely, i.e. to fit each other, also enhances ligand binding.

With the exception of the modelled Common carp and Chinese perch lysozyme structures, GEWL and the other models have a net negative charge at the active site, more so in Atlantic salmon and Takifugu rubripes because of the N122E substitution. Two particular substitutions, D86P and N122H in the carp and perch proteins, respectively, neutralise the net charge of the corresponding active site. This, coupled with the knowledge that the main interacting residue on Ivy is a positively charged His60, seems to rule out electrostatic incompatibility as a reason for the lack of inhibition.

Similar to all vertebrates investigated, salmonids have genes for, and express, lysozymes of both *c*- and *g*-types. It

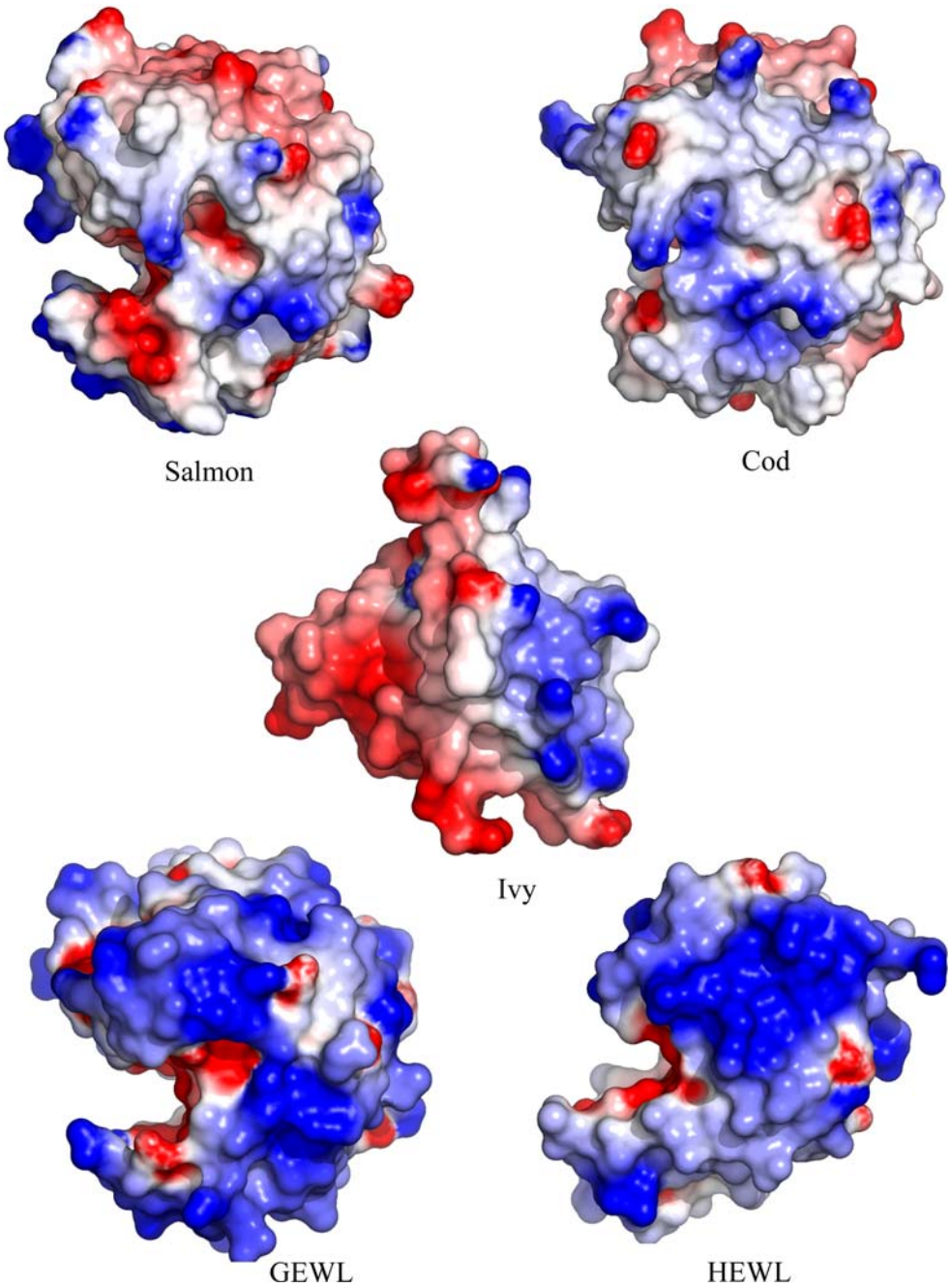

Fig. 8 Electrostatic surface potentials of Ivy, HEWL and GEWL and the cod and salmon *g*-type lysozyme models in a slice plane containing the molecular surface of the protein–inhibitor interaction. The colour runs from *intense red* (lowest) to intense *blue* (highest) potential

Table 3 Salt bridges in vertebrate lysozyme (Ivy)/hen egg white lysozyme (HEWL) and Ivy/GEWL complexes

Ivy atom	HEWL atom	Atomic distance (Å)	GEWL atom	Atomic distance (Å)
ND1 H60	OE1 E35	2.71	OE1 E73	2.97
OD2 D3	NH2 R45	3.12		
OD2 D61	NH1 R114	3.06	ND1 H75	3.78
OE2 E87			NZ K78	3.06
NZ K58			OE1 E24	2.72
NZ K34			OD1 D167	2.6

is still quite unclear why two different sets of genes that produce antibacterial enzymes displaying similar activity have evolved. However, in contrast to the lack of inhibition of the salmon *g*-type lysozyme reported here, salmonid *c* lysozymes are subjected to inhibition by Ivy from *E. coli* (I.W. Nilsen and B. Myrnes; unpublished data). Thus, the *c*- and *g*-types may in some ways be regarded as mutual back-ups in the innate immune system. Aquatic and terrestrial environments differs strongly from each other in nature, in particular by the continuous exposure to high concentrations of bacteria in the sea or freshwater. This may have resulted in the development of an efficient and

(compared to terrestrial vertebrates) less fragile fish antibacterial defence system that is less vulnerable to, for instance, bacterial inhibitors of lysozymes. The same rationality may be applied to marine invertebrates, many of which are filter-feeders, meaning that they need peptidoglycan-hydrolysing enzymes for defence against bacteria as well as for processing bacteria for feeding. Supportive of this idea, our previous work showed that activities of neither *g*-type lysozyme of the tunicate *O. dioica* nor of *i*-type lysozyme of the scallop *Chlamys islandica*, both supposedly the only lysozyme-types of their species, were negatively affected by Ivy [8, 10].

Summary

In the present study, we have investigated possible inhibition of fish *g*-type lysozymes by Ivy using homology modelling, protein–protein docking as well as functional enzyme assays. Computational modelling revealed that these aquatic lysozymes have altered surface characteristics when compared to GEWL, which possibly result in lack of inhibition by Ivy. Strong inhibition of HEWL and GEWL by Ivy has previously been observed experimentally, but our model of Ivy bound to GEWL differs significantly from the crystal structure of Ivy–HEWL. Nevertheless, the principal properties of the Ivy–HEWL complex are maintained in Ivy–GEWL, as key interactions mediated by the CKPHDC loop of Ivy persist in the modelled structure. Further support for the modelling presented is added by the enzyme inhibition studies, which demonstrate that *g*-type lysozyme from salmon is not inhibited by Ivy.

Acknowledgements This work was supported by the Norwegian Research Council (NFR), the Norwegian Institute of Fisheries and Aquaculture Research, Tromsø (Fiskeriforskning) and the Norwegian Structural Biology Centre (NorStruct) at the University of Tromsø. Recombinant Ivy was a kind gift from Professor Chris Michiels at the Catholic University of Leuven, Belgium.

References

1. Flemming A (1922) Proc R Soc London, Ser B 39:306–317
2. Jolles P, Jolles J (1984) Mol Cell Biochem 63:165–189
3. Jollès P (1996) Lysozymes: Model enzymes in biochemistry and biology. Birkhäuser, Basel
4. Wild P, Gabrieli A, Schraner EM, Pellegrini A, Thomas U, Frederik PM, Stuart MCA, VonFellenberg R (1997) Microsc Res Tech 39:297–304
5. Canfield RE, McMurry S (1967) Biochem Biophys Res Commun 26:38–42
6. Hikima J, Minagawa S, Hirono I, Aoki T (2001) Biochim Biophys Acta 1520:35–44
7. Irwin DM, Gong Z (2003) J Mol Evol 56:234–242
8. Nilsen IW, Myrnes B, Edvardsen RB, Chourrout D (2003) Cell Mol Life Sci 60:2210–2218
9. Jolles J, Jolles P (1975) Eur J Biochem 54:19–23
10. Nilsen IW, Overbo K, Sandsdalen E, Sandaker E, Sletten K, Myrnes B (1999) FEBS Lett 464:153–158
11. Nilsen IW, Myrnes B (2001) Gene 269:27–32
12. Bachali S, Jager M, Hassanin A, Schoentgen F, Jolles P, Fiala-Medioni A, Deutsch JS (2002) J Mol Evol 54:652–664
13. Weaver LH, Grutter MG, Remington SJ, Gray TM, Isaacs NW, Matthews BW (1984) J Mol Evol 21:97–111
14. Grinde B (1989) FEMS Microbiol Lett 60:179–182
15. Monchois V, Abergel C, Sturgis J, Jeudy S, Claverie JM (2001) J Biol Chem 276:18437–18441
16. Fernie-King BA, Seilly DJ, Davies A, Lachmann PJ (2002) Infect Immun 70:4908–4916
17. Callewaert L, Aertsen A, Deckers D, Michiels CW (2006) Commun Appl Biol Sci 71:87–90
18. Abergel C, Monchois V, Byrne D, Chenivesse S, Lembo F, Lazzaroni JC, Claverie JM (2007) Proc Natl Acad Sci USA 104:6394–6399
19. Deckers D, Masschalck B, Aertsen A, Callewaert L, Van Tiggelen CG, Atanassova M, Michiels CW (2004) Cell Mol Life Sci 61:1229–1237
20. Lukomski S, Hoe NP, Abdi I, Rurangirwa J, Kordari P, Liu MY, Dou SJ, Adams GG, Musser JM (2000) Infect Immun 68:535–542
21. Fernie-King BA, Seilly DJ, Lachmann PJ (2004) Immunol 111:444–452
22. Callewaert L, Masschalck B, Deckers D, Nakimbugwe D, Atanassova M, Aertsen A, Michiels CW (2005) Enzyme Microb Technol 37:205–211
23. Callewaert L, Masschalck B, Aertsen A, Michiels CW (2005) Commun Appl Biol Sci 70:73–87
24. Kyomuhendo P, Myrnes B, Nilsen IW (2007) Cell Mol Life Sci 64:2841–2847
25. Bairoch A, Apweiler R, Wu CH, Barker WC, Boeckmann B, Ferro S, Gasteiger E, Huang H, Lopez R, Magrane M, Martin MJ, Natale DA, O'Donovan C, Redaschi N, Yeh LS (2005) Nucleic Acids Res 33:D154–159
26. Notredame C, Higgins DG, Heringa J (2000) J Mol Biol 302: 205–217
27. Boguski MS, Lowe TM, Tolstoshev CM (1993) Nat Genet 4: 332–333
28. Hall T (1999) Nucleic Acids Symp Ser 41:95–98
29. Saitou N, Nei M (1987) Mol Biol Evol 4:406–425
30. Felsenstein J (1989) Cladistics 5:164–166
31. Felsenstein J (1985) Evolution 39:783–791
32. Berman HM, Westbrook J, Feng Z, Gilliland G, Bhat TN, Weissig H, Shindyalov IN, Bourne PE (2000) Nucleic Acids Res 28:235–242
33. Abagyan R, Totrov M, Kuznetsov D (1994) J Comput Chem 15:488–506
34. Jaroszewski L, Pawlowski K, Godzik A (1998) J Mol Model 4:294–309
35. Luthy R, Bowie JU, Eisenberg D (1992) Nature 356:83–85
36. Colovos C, Yeates TO (1993) Protein Sci 2:1511–1519
37. Laskowski RA, Macarthur MW, Moss DS, Thornton JM (1993) J Appl Crystallogr 26:283–291
38. Hooft RWW, Vriend G, Sander C, Abola EE (1996) Nature 381:272–272
39. Schneidman-Duhovny D, Inbar Y, Polak V, Shatsky M, Halperin I, Benyamini H, Barzilai A, Dror O, Haspel N, Nussinov R, Wolfson HJ (2003) Proteins Struct Funct Genet 52:107–112
40. Guex N, Peitsch MC (1997) Electrophoresis 18:2714–2723
41. Pearlman DA, Case DA, Caldwell JW, Ross WS, Cheatham TE, Debolt S, Ferguson D, Seibel G, Kollman P (1995) Comput Phys Commun 91:1–41

42. Berendsen HJC, Postma JPM, Vangunsteren WF, Dinola A, Haak JR (1984) J Chem Phys 81:3684–3690
43. Darden T, York D, Pedersen L (1993) J Chem Phys 98:10089–10092
44. Ryckaert JP, Ciccotti G, Berendsen HJC (1977) J Comput Phys 23:327–341
45. Weaver LH, Grutter MG, Matthews BW (1995) J Mol Biol 245:54–68
46. Grütter MG, Weaver LH, Matthews BW (1983) Nature 303:828–831
47. Drozdov-Tikhomirov LN, Linde DM, Poroikov VV, Alexandrov AA, Skurida GI (2001) J Biomol Struct Dyn 19:279–284
48. Honig B, Nicholls A (1995) Science 268:1144–1149